Transverse-energy-energy correlations in deep inelastic scattering

Hai Tao Li,[a] **Ivan Vitev**[a] **and Yu Jiao Zhu**[b]

[a]*Los Alamos National Laboratory, Theoretical Division,*
Los Alamos, NM 87545, U.S.A.

[b]*Zhejiang Institute of Modern Physics, Department of Physics, Zhejiang University,*
Hangzhou 310027, China

E-mail: haitaoli@lanl.gov, ivitev@lanl.gov, zhuyujiao@zju.edu.cn

ABSTRACT: Event shape observables have been widely used for precision QCD studies at various lepton and hadron colliders. We present the most accurate calculation of the transverse-energy-energy correlation event shape variable in deep-inelastic scattering. In the framework of soft-collinear effective theory the cross section is factorized as the convolution of the hard function, beam function, jet function and soft function in the back-to-back limit. A close connection to TMD factorization is established, as the beam function when combined with part of the soft function is identical to the conventional TMD parton distribution function, and the jet function is the second moment of the TMD fragmentation function matching coefficient. We validate our framework by comparing the obtained LO and NLO leading singular distributions to the full QCD calculations in the back-to-back limit. We report the resummed transverse-energy-energy correlation distributions up to N³LL accuracy matched with the NLO cross section for the production of a lepton and two jets. Our work provides a new way to precisely study TMD physics at the future Electron-Ion Collider.

Contents

1 Introduction

Event shape observables describe the patterns, correlations, and energy flow of hadronic final states in high energy processes. They have been widely investigated to study the various dynamical aspects of QCD in e^+e^-, ep, pp, and heavy-ion collisions. Event shape variables can be used to determine the strong coupling α_s and test asymptotic freedom, to tune the nonperturbative Quantum Chromodynamics (QCD) power corrections, and to search for new physics phenomena. Furthermore, these observables can be studied with high precision theoretically and compared to experimental measurements at the future Electron-Ion Collider (EIC).

There are many efforts devoted to the study of event shape observables in deep-inelastic scattering (DIS). The next-to-leading order (NLO) QCD corrections were obtained about twenty years ago [1–3]. Recently, the next-to-next-to-leading order (NNLO) QCD corrections to various event shape distributions were computed in ref. [4]. Near the infrared region resummation is required to obtain reliable predictions, which are available at next-to-leading logarithmic (NLL) level [5–8] for most event shape observables, next-to-next-to-leading logarithmic (NNLL) level for 1-jettiness [9] and angularity [10], and next-to-next-to-next-to-leading logarithmic (N^3LL) level for thrust [11]. On the experimental side, H1 and ZEUS collaborations have measured some event shape variables at HERA [12–17]. With more precise measurements in DIS at the future EIC, event shape observables can serve as a precision test of QCD and new probes to reveal the proton or nuclear structure.

Here, we will concentrate on the transverse-energy-energy correlation (TEEC) event shape observable in DIS. TEEC [18] at hadronic colliders is an extension of the energy-energy correlation (EEC) [19] variable introduced decades ago in e^+e^- collisions to describe

the global event shape. The EEC is defined as

$$\text{EEC} = \sum_{a,b} \int d\sigma_{e^+e^- \to a+b+X} \frac{2E_a E_b}{|\sum_i E_i|^2} \delta(\cos\theta_{ab} - \cos\theta) \,, \tag{1.1}$$

where E_i is the energy of hadron i and θ_{ab} is the opening angle between hadrons a and b. New studies of EECs, which include analytical NLO calculations [20, 21], NNLO in $\mathcal{N} = 4$ super-Yang-Mills theory [22–25], all-order factorization in QCD in the back-to-back limit [26], and all order structure in the collinear limit [27–30], have furthered our understanding of this observable.

At hadronic colliders, where detectors lack the typical hermeticity of detectors at e^+e^- machines, the event shape observable can be generalized by considering the transverse energy of the hadrons. TEEC, which is defined as

$$\text{TEEC} = \sum_{a,b} \int d\sigma_{pp \to a+b+X} \frac{2E_{T,a} E_{T,b}}{|\sum_i E_{T,i}|^2} \delta(\cos\phi_{ab} - \cos\phi) \,, \tag{1.2}$$

was investigated in refs. [31–33]. In eq. (1.2) $E_{T,i}$ is the transverse energy of hadron i and ϕ_{ab} is the azimuthal angle between hadrons a and b. The NLO QCD corrections for the TEEC observable were calculated in ref. [31]. The works [32, 33] investigated TEEC in the dijet limit and showed that it exhibits remarkable perturbative simplicity.

In DIS, TEEC can be generalized by considering the transverse-energy and transverse-energy correlation between the lepton and hadrons in the final state, which is first studied in this work. We define this event shape observable as follows:

$$\begin{aligned} \text{TEEC} &= \sum_{a} \int d\sigma_{lp \to l+a+X} \frac{E_{T,l} E_{T,a}}{E_{T,l} \sum_i E_{T,i}} \delta(\cos\phi_{la} - \cos\phi) \\ &= \sum_{a} \int d\sigma_{lp \to l+a+X} \frac{E_{T,a}}{\sum_i E_{T,i}} \delta(\cos\phi_{la} - \cos\phi) \,, \end{aligned} \tag{1.3}$$

where the sum runs over all the hadrons in the final states and ϕ_{la} is the azimuthal angle between final state lepton l and hadron a. Note that there is no QCD collinear singularity ($\phi_{la} \to 0$) along the outgoing lepton's momentum in DIS, for which one needs to perform the resummation at hadron colliders and in e^+e^- annihilation [27]. As we will show below, resummed predictions in the back-to-back limit ($\phi_{la} \to \pi$) can be obtained to high accuracy and the distribution in the whole range $\phi \in [0, \pi]$ can be reliably calculated. One of the advantages of EEC/TEEC is that the contribution from soft radiation is suppressed as it carries parametrically small energy. Therefore, the hadronization effects are expected to be small in comparison to other event shape observables. TEEC in DIS can be used to determine the strong coupling precisely similar to analysis in refs. [1–3] and to study the nuclear dynamic as in ref. [9]. Additionally it is also feasible to study transverse-momentum dependent (TMD) physics using TEEC in DIS.

In this paper, we present our study of TEEC in the DIS process. Similar to EEC [26] in e^+e^- collisions and TEEC [32] in hadronic collisions, the cross section for this observable in the back-to-back limit can be factorized as the convolution of the hard function, beam

function, jet function, and soft function using the frameworks of soft-collinear effective theory (SCET) [34–38]. This approach is similar to a 1-dimension TMD factorization and is, thus, closely related to TMD physics. The beam functions are identical to the TMD parton distribution functions (PDFs) and the jet function is the second moment of the matching coefficients of the TMD fragmentation functions. For details see refs. [26, 39, 40]. Furthermore, the factorization formalism is also similar to the usual TMD factorization, for example see the work [41] for N^3LL jet q_T distribution. The non-trivial LO and NLO QCD distributions of the TEEC observable are reproduced by the leading power SCET in the back-to-back limit, which validates our formalism. Resummation can be achieved by evolving each component of the factorized expression from its intrinsic scale to a suitably chosen common scale. The main goal of our work is to present the most precise TEEC predictions in DIS at $N^3LL+NLO$. The effects of the nonperturbative physics are also discussed. Since there is no collinear singularity, we are able to provide the $N^3LL+NLO$ distribution in the complete range of $0 < \phi < \pi$. The perturbative behavior of this observable is under good theoretical control in QCD, which can be further improved if one can match the resummation with NNLO corrections. Consequently, it can be used to study the non-perturbative physics in a precise quantitative manner.

The rest of this paper is organized as follows. In the next section the factorization formalism for the TEEC observable is present. The hard function, beam function, jet function, and soft function are discussed. In section 3 we investigate the hadronization effect using PYTHIA8. We further verify the factorization formula by comparing the LO and NLO singular distribution with the full QCD ones. The N^3LL and $N^3LL+NLO$ predictions are also present. Finally, we conclude in section 4. The RG equations and anomalous dimensions are present in appendix A.

2 Theoretical formalism

The underlying partonic Born process considered in this work is

$$e(k_1) + q(k_2) \to e(k_3) + q(k_4). \tag{2.1}$$

The first order non-trivial contribution to TEEC begins from one order higher. In the back-to-back limit, the TEEC cross section is defined as

$$\frac{d\sigma}{d\cos\phi} \approx \sum_h \int d\sigma_{lN \to l+h+X} \times \frac{p_T^h}{p_T} \times \delta(\cos\phi_{lh} - \cos\phi), \tag{2.2}$$

where p_T is the transverse momentum of the outgoing lepton. We define the momenta of the event in the $x - z$ plane, i.e. at LO the components of all the momenta along y-direction are zero. In the back-to-back limit it is convenient to introduce the variable $\tau = (1+\cos\phi)/2$, related to the non-zero momentum balance along y-direction of the event due to soft and/or collinear radiations. It can be written as

$$\tau = \frac{\left| k_{2,y} - k_{s,y} + \frac{k_{4,y}}{\xi_4} \right|^2}{4p_T^2}, \tag{2.3}$$

– 3 –

where $k_{s,y}$ is the y-momentum of the soft radiation and ξ_4 is the momentum fraction of the hadron relative to the jet. The soft radiation contributes through the recoil to the energetic collinear partons. Similar to the case of EEC in electron-position collisions or TEEC at hadronic collisions, the cross section in the back-to-back limit is factorized into the convolution of a hard function, beam function, soft function, and jet function. Specifically, up to leading power in SCET the cross section can be written as

$$\frac{d\sigma^{(0)}}{d\tau} = \sum_f \int \frac{d\xi dQ^2}{\xi Q^2} Q_f^2 \sigma_0 \frac{p_T}{\sqrt{\tau}} \int \frac{db}{2\pi} e^{-2ib\sqrt{\tau}p_T} B_{f/N}(b, E_2, \xi, \mu, \nu) H(Q, \mu)$$
$$\times S\left(b, \frac{n_2 \cdot n_4}{2}, \mu, \nu\right) J_f(b, E_4, \mu, \nu) , \tag{2.4}$$

where $\sigma_0 = \frac{2\pi\alpha^2}{Q^2}[1 + (1-y)^2]$, b is the conjugate variable to k_y, Q^2 is the invariant mass of the virtual photon, and $y = Q^2/\xi/s$. Four-vectors n_2 and n_4 represent the momentum directions of the momenta k_2 and k_4, respectively. E_2 and E_4 are the energies of k_2 and k_4. ν is rapidity scale associated with the rapidity regulator for which we adopt the exponential regulator introduced in ref. [42].

$B_{f/N}$, which describe the contribution from collinear radiation in the initial state, are the same as the usual TMD beam functions. The operator definition for the beam function in SCET is

$$B_{q/N}(b, \xi) \equiv \int \frac{db}{4\pi} e^{-i\xi b P^+/2} \left\langle N(P) \left| \bar{\chi}_n\left(0, b^-, b_\perp\right) \frac{\not{n}}{2} \chi_n(0) \right| N(P) \right\rangle , \tag{2.5}$$

with $\chi_n = W_n^\dagger \xi_n$, where ξ_n is the collinear quark field and W_n is the path-ordered collinear Wilson line $W_n(x) = \mathcal{P} \exp\left(ig \int_{-\infty}^0 ds\bar{n} \cdot A_n(x + \bar{n}s)\right)$. In the operator definition, we suppress the arguments of kinematics and scales. The TMD beam functions have been calculated up to three loops for quark beam functions and two loops for gluon beam functions [39, 40, 43–47].

The jet functions J_f are defined as the second Mellin moment of the matching coefficients of the TMD fragmentation function [39, 40, 46, 48]. The explicit expression up to two loops for the jet functions can be found in refs. [39, 40].

The operator definition for the soft function is

$$S_{\text{DIS}}(b) \equiv \frac{1}{N_c} \text{Tr} \left\langle 0 \left| \bar{T}\left[Y_{n_2}(0)Y_{n_4}^\dagger(0)\right]^\dagger T\left[Y_{n_2}(0)Y_{n_4}^\dagger(0)\right] \right| 0 \right\rangle , \tag{2.6}$$

where Y_{n_2} and $Y_{n_4}^\dagger$ correspond to an incoming quark and an outgoing quark, respectively. The explicit expressions of Y_{n_2} and $Y_{n_4}^\dagger$ are

$$Y_{n_2}(x) = \mathcal{P} \exp\left(ig_s \int_{-\infty}^0 dsn_2 \cdot A_s(x + sn_2)\right) ,$$
$$Y_{n_4}^\dagger(x) = \mathcal{P} \exp\left(ig_s \int_0^\infty dsn_4 \cdot A_s(x + sn_4)\right) . \tag{2.7}$$

We suppress the arguments of kinematics and scales in the operator definition. The soft function for TEEC in DIS can be written in terms of the soft function in EEC in e^+e^-

collisions, which can be written as

$$S\left(b, \frac{n_2 \cdot n_4}{2}, \mu, \nu\right) = S_{\text{EEC}}\left(L_b, L_\nu + \ln\frac{n_2 \cdot n_4}{2}\right), \tag{2.8}$$

where S_{EEC} is the soft function for EEC. In the above $L_\nu = \ln \nu^2 b^2/b_0^2$ and $L_b = \ln \mu^2 b^2/b_0^2$ with $b_0 = 2e^{-\gamma_E}$. S_{EEC} is identical to TMD soft function [26]. Up to three loops the expression for the soft function can be found in refs. [49].

The hard function encodes the short-distance physics, which is the matching coefficient from full QCD onto SCET. The analytical expression of $H(Q, \mu)$ up to NNLO is given in ref. [50] and the one at three-loop level can be obtained from the quark form factor, as shown in refs. [51, 52].

The renormalization group (RG) equations and anomalous dimensions needed for our calculation are given in appendix A. With all the components and their RG equations available, we can achieve precision predictions for this observable up to N^3LL. The resummed cross section is obtained by evolving the hard function from μ_h to μ_c and the soft function from (μ_s, ν_s) to (μ_c, ν_c). It can be written as

$$\frac{d\sigma_{\text{RES}}^{(0)}}{d\tau} = \sum_f \int \frac{d\xi dQ^2}{\xi Q^2} Q_f^2 \sigma_0 \frac{p_T}{\sqrt{\tau}} \int \frac{db}{2\pi} e^{-2ib\sqrt{\tau}p_T} B_{f/N}(b, E_2, \xi, \mu_c, \nu_c) H(Q, \mu_h)$$

$$\times S\left(b, \frac{n_2 \cdot n_4}{2}, \mu_s, \nu_s\right) J_f(E_4, b, \mu_c, \nu_c) \exp\left[\int_{\mu_h}^{\mu_c} \frac{d\bar{\mu}}{\bar{\mu}} \Gamma_h(\bar{\mu}) + \int_{\mu_s}^{\mu_c} \frac{d\bar{\mu}}{\bar{\mu}} \Gamma_s(\bar{\mu}, \nu_s)\right]$$

$$\times \exp\left[\int_{\nu_s}^{\nu} \frac{d\bar{\nu}}{\bar{\nu}} \Gamma_r(\mu_c, \mu_b)\right], \tag{2.9}$$

where Γ_h and Γ_s are the anomalous dimensions of the hard and soft functions, and Γ_r is the rapidity anomalous dimension of the soft function.

The prediction away from the back-to-back limit is obtained through matching the resummed calculations with the fixed-order ones, which can be written as

$$\frac{d\sigma_{\text{N}^l\text{LL}+\text{N}^k\text{LO}}}{d\tau} = \frac{d\sigma_{\text{N}^l\text{LL}}}{d\tau} + \frac{d\sigma_{\text{N}^k\text{LO}}}{d\tau} - \left(\frac{d\sigma_{\text{N}^k\text{LO}}}{d\tau}\right)_{\text{sing.}}. \tag{2.10}$$

The singular distribution $\left(\frac{d\sigma_{\text{N}^k\text{LO}}}{d\tau}\right)_{\text{sing.}}$ is the fixed-order prediction from eq. (2.4) in the leading power of SCET, which captures the singular behavior of the QCD fixed-order predictions in the leading power in the back-to-back limit.

3 Numerical results

We will present numerical predictions with enter-of-mass energy $\sqrt{s} = 141\,\text{GeV}$, corresponding to beam energies 20 (lepton) $\text{GeV} \times 250$ (proton) GeV, typical for the future EIC [53]. We also consider enter-of-mass energy $\sqrt{s} = 318\,\text{GeV}$, corresponding to beam energies $27.5\,\text{GeV} \times 920\,\text{GeV}$ at HERA. We select events with constraints on the transverse momentum of the outgoing lepton $p_T^l > 20\,\text{GeV}$ and $p_T^l > 30\,\text{GeV}$ for 141 GeV and 318 GeV electron-proton collisions, respectively. All calculations are performed using PDF4LHC15_nnlo_mc PDF sets [54–57] and the associated strong coupling provided by LHAPDF6 [58].
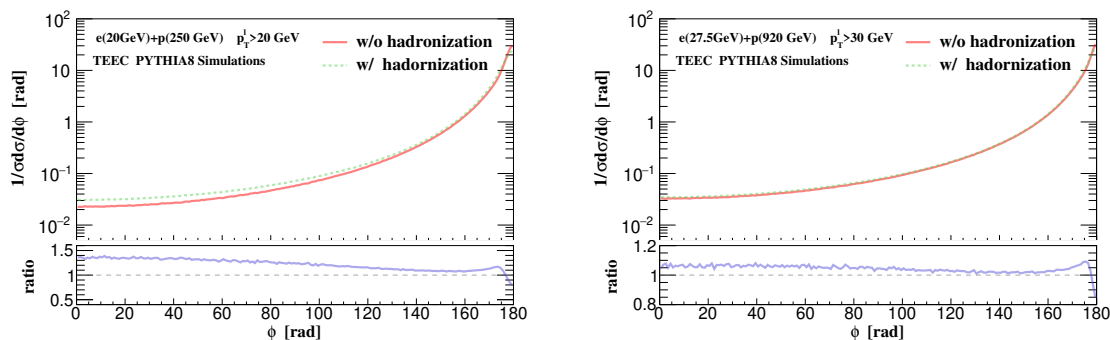
Figure 1. PYTHIA simulations of the TEEC distribution versus ϕ with and without hadronization effects. We consider center-of-mass energy $\sqrt{s} = 141\,\text{GeV}$ with $p_T^l > 20\,\text{GeV}$ (left), and enter-of-mass energy $\sqrt{s} = 318\,\text{GeV}$ with $p_T^l > 30\,\text{GeV}$ (right). The ratio is defined as predictions with hadronization effects divided by the ones without hadronization effects.

3.1 PYTHIA **simulation**

To assess the effects of hadronization on the TEEC observable we start with PYTHIA8 [59, 60] simulations. Figure 1 shows the predictions for normalized TEEC with and without hadronization in $\sqrt{s} = 141$ Gev (left) and $\sqrt{s} = 318\,\text{GeV}$ (right) ep collisions. The lepton is selected with a finite transverse momentum in the final state and there is no divergence in the usual collinear limit ($\phi \to 0^o$). The cross section is dominated by the back-to-back region, where there are collinear and/or soft singularities in fixed-order calculations. As shown in figure 1, the hadronization effects are more important in $\sqrt{s} = 141\,\text{GeV}$ ep collisions since the tagged lepton is of a smaller p_T. The corrections themselves are about 20 to 35 percent for small and large ϕ. For $\sqrt{s} = 318$ GeV collisions the hadronization effects are a few percent for small ϕ and about 15% in the back-to-back region. In comparison to other event shape observables, as can be seen in the simulations in ref. [4], the overall hadronization effects are much smaller. The reason behind this observation is that the soft particle contribution is suppressed by the energy in the TEEC. Therefore, the predictions for the TEEC observable can be significantly improved through high order calculations in perturbative QCD. In this section we will show that N^{3}LL TEEC in the back-back limit is under very good control after resummation and the nonperturbative effects are investigated. In the future the distributions can be further improved with NNLO calculations. Subsequently, the observable can be used to test perturbative QCD and measure the QCD coupling in a unique way.

3.2 **Fixed-order results**

We now move on to the core calculations in our work on TEEC in DIS. In figure 2 we present the comparison of the leading singular distributions from SCET to full QCD calculations. Figure 2 also shows the non-singular contributions which are defined as the differences between the full QCD and the singular calculations. With the known components in eq. (2.4) up to two loops, the LO and δNLO singular distributions are present with solid orange and solid green lines. With three-loop anomalous dimensions the singular
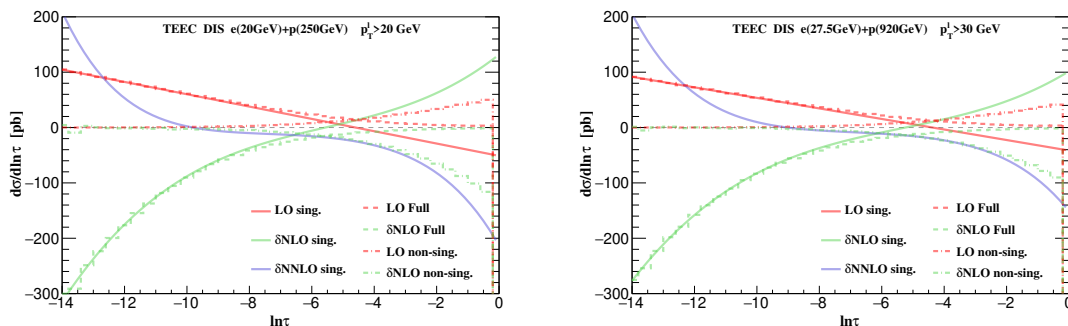
Figure 2. Fixed-order results for the $\ln\tau$ distributions in the back-to-back limit for $\sqrt{s} = 141\,\mathrm{GeV}$ (left) and $318\,\mathrm{GeV}$(right) ep collisions. The full QCD (dash lines) and non-singular (dash-dotted lines) distributions are shown up to NLO, while the leading singular (solid lines) distributions are up to NNLO.
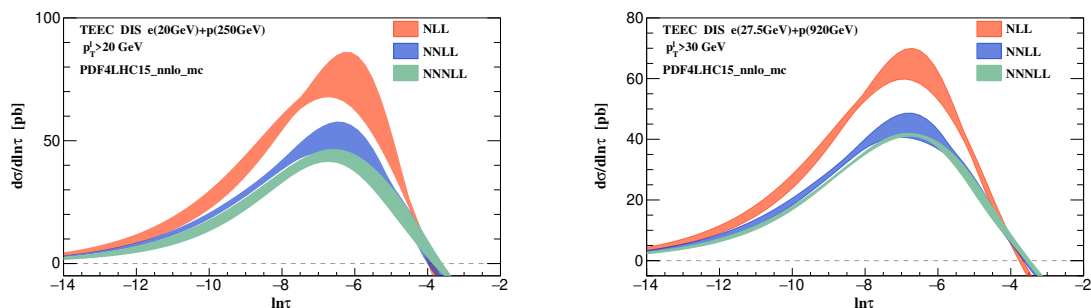

Figure 3. Resummed distributions in the back-to-back limit. The orange, blue, and green bands are the predictions with scale uncertainties at NLL, NNLL and N³LL, respectively. Left and right panels are for EIC and HERA energies, respectively.

distributions are calculated up to NNLO in QCD and are shown as the solid blue lines. The singular distributions oscillate between ∞ and $-\infty$ from LO to NNLO when $\tau \to 0$. The full LO and NLO results for two jet production in DIS are calculated making use of Nlojet++ [3, 61] and are denoted by dashed lines. Finally, the dash-dotted lines stand for the non-singular distributions. The renormalization and factorization scales are set to be $\mu = Q$. The LO and NLO singular distributions from SCET perfectly reproduce the full QCD results in the back-to-back limit, which provides a solid check of our factorization formalism. In the range $\tau \to 1$, the factorization formula does not work well and there are large power corrections, as expected. For small τ the logarithmic structures in the singular distributions needed to be resummed to all orders in α_s to obtain stable predictions.

3.3 Resummed predictions

We set the default scales in our calculation to $\mu_h = \nu = Q$, $\mu_s = \mu = \nu_s = \mu_b$. The scale uncertainties are defined as the quadratic sum over the results when we vary μ_h, μ_s, μ, ν_s and ν independently by a factor of two around their default values. To avoid Landau pole we use the b^* prescription [62] and define $b^* = b/\sqrt{1 + b^2/b_{\max}^2}$. We further define
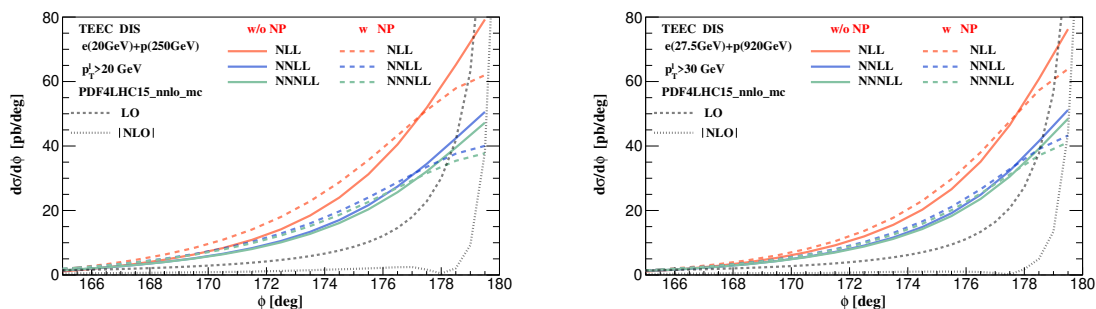
Figure 4. Nonperturbative effects for NLL (orange), NNLL (blue) and N³LL (green) TEEC distributions in DIS. The solid and dashed lines are the predictions without and with nonperturbative effects, respectively.
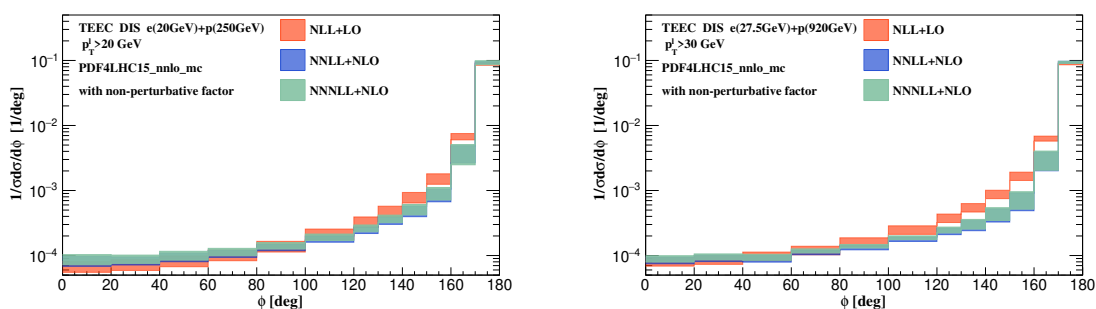

Figure 5. The TEEC ϕ distribution matched with a nonperturbative model. The orange, blue and green bands are the final predictions with scale uncertainties at NLL+LO, NNLL+NLO, and N³LL+NLO, respectively.

$\mu_b = b_0/b^*$ and set $b_{\max} = 1.5\,\text{GeV}^{-1}$. For completeness, we varied the nonperturbative parameter $1\,\text{GeV}^{-1} < b_{\max} < 2\,\text{GeV}^{-1}$. We found that the dependence on $b_{\max}$ of the resummed distributions is very small.

Figure 3 presents the resummed predictions at NLL, NNLL, and N³LL accuracy in the back-to-back limit with scale uncertainties. We find very good perturbative convergence. There is about 30% suppression in the peak region from NLL to NNLL, while it is about 5-6% from NNLL to N³LL. The scale uncertainty of the N³LL result is larger for 141 GeV ep collisions, and is around 12% near the peak. For 318 GeV collisions the uncertainty is only about 2%. The factorization formula gives more accurate predictions at $\sqrt{s} = 318\,\text{GeV}$ due to larger scale hierarchy. In both cases the uncertainties are significantly improved order-by-order. The resummed distributions turn negative when $\tau \to 1$ where the effective theory becomes invalid.

In general the nonperturbative (NP) corrections can be important in the infrared region. For EEC in e^+e^- collisions, the work [63] investigated the nonperturbative effects in detail using α_{eff} and a power corrections scheme. However, we use a different approach, the b^* prescription, commonly found in hadron collider phenomenology to deal with the Landau pole. The nonperturbative effects for TEEC in DIS are related to initial state

PDFs, or beam functions, which is different in comparison with the case of EEC. In this work choose the non-perturbative model used in q_T resummation with parameters obtained through fitting data from refs. [64, 65]. The nonperturbative effects are included by a multiplicative factor in eq. (2.9)

$$S_{\mathrm{NP}} = \exp\left[-0.106\ b^2 - 0.84\ln Q/Q_0 \ln b/b^*\right]\ , \tag{3.1}$$

with $Q_0 = 1.55\,\mathrm{GeV}$. Figure 4 shows the effect of the nonperturbative factor, where the solid and dashed lines are the predictions without and with the NP factor, respectively. The nonperturbative factor suppresses the cross section for $\phi \sim 180^o$ where low-energy physics is important. The nonperturbative effects are larger in 141 GeV collisions when compared to those in 318 GeV collisions because the corresponding cross section in 141 GeV collisions has a smaller intrinsic scale. Figure 4 also includes the $d\sigma_{\mathrm{LO}}/d\phi$ and $|d\sigma_{\mathrm{NLO}}/d\phi|$,[1] which are represented by gray dashed and dotted lines. The fixed-order predictions are divergent when $\phi \to 180^o$ as expected. Resummation improves these predictions considerably.

Eq. (3.1) is not the only possible form of nonperturbative corrections. For example, for EEC, the work [63] considered both a quadratic and a linear contributions in the impact parameter b. The latter can arise from correlations between quarks and soft gluons emitted at the scale of order Λ_{QCD} and can give a dominant contribution to the NP effects. A study along those lines in the future can help us better understand the interplay between the perturbative and non-perturbative corrections in the back-to-back region.

The results for the normalized TEEC ϕ distributions are shown in figure 5, where the nonperturbative factor from eq. (3.1) is also implemented. The matching region is chosen to be $160^o < \phi < 175^o$ and for $\phi < 160^o$ the distributions are generated by fixed-order calculations. The fixed-order predictions are calculated with $\mu_r = \mu_f = \kappa Q$ with $\kappa = (0.5, 1, 2)$. In the back-to-back limit, the predictions are significantly improved. For the second to last bin in figure 5 where $\phi \approx 165^o$ or $\ln\tau \approx -4.1$, the non-singular contributions are large, which is consistent with figure 2 and figure 3. The scale uncertainties are dominated by the non-singular terms. The scale uncertainties for the normalized distributions at NNLL+NLO and N³LL+NLO are dominated by the NLO calculations away from the back-to-back region. Because of accidental cancellation of the scale dependence for the normalized TEEC distributions at LO, it seems that the NLO QCD corrections do not reduce the scale uncertainties. However, as documented in ref. [4], the NNLO QCD corrections are expected to reduce the scale dependence of event shape observables significantly. Therefore, we expect that matching with NNLO QCD calculations will further reduce the scale uncertainties, but is beyond the scope of this paper. The resummation improves the prediction significantly for $\phi \sim 180^o$. There is a small difference for $\phi < 160^o$ between NNLL+NLO and N³LL+NLO because in a normalized distribution changes in a few bins will affect the distribution in the whole plotted range.

---

[1]The NLO cross section turns negative when ϕ is very close to 180°.

4 Conclusion

In this paper, we carried out the first study on TEEC in DIS. In the back-to-back limit the TEEC cross section can be factorized into the product of the hard function, beam function, jet function, and soft function in position space — closely related to the ordinary TMD physics. We validated the formalism by comparing our LO and NLO singular distributions to the full QCD calculations in the back-to-back limit. The NNLO singular distribution is also provided as a future cross-check of the NNLO cross section for $e + p \rightarrow e+2\text{jet}$. The resummed distributions were obtained through solving the RG equations for each component. We found very good perturbative convergence and the scale uncertainties were significantly reduced order-by-order. The nonperturbative effects were assessed using PYTHIA simulations and a nonperturbative model widely used in q_T resummation. Importantly, we presented the first theoretical prediction for ϕ distributions at N^{3}LL+NLO accuracy. In the future it will be interesting to consider on the perturbative side matching to an NNLO fixed order calculation [4]. On the nonperturbative side one can explore corrections that arise from quark-gluon correlations and might have a different functional form [63] than the ones included here.

The EEC/TEEC event shape observables can be studied in e^+e^-, ep and pp collisions, which provides a way to test the universality of QCD factorization in different colliding systems. These observables can also be used to study TMD physics, which is one of the most important goals of the EIC. Finally, we remark that TEEC can also be used to shed light on the interaction between partons and a QCD medium in electron-ion (eA) or ion-ion (AA) collisions. Ongoing theoretical and experimental design efforts aim to elucidate the physics opportunities with hadron and jet modification at the EIC and, very importantly, to ensure that the detectors at this future facility have the capabilities to perform the necessary measurements, see e.g. ref. [66].

As our calculations rely on the SCET framework, a natural choice to address TEEC in eA collisions is the extension of the effective theory approach to include the interactions between partons and the background QCD medium mediated by Glauber gluons. Soft collinear effective theory with Glauber gluon interactions has provided a mean to evaluate the contribution in-medium parton showers [67, 68] to a variety of observables in reactions with nuclei. The most recent examples include the modification of jet cross sections and jet substructure ranging from the jet splitting functions to the jet charge [69–71]. To obtain predictions for the TEEC event shape observable in DIS on nuclei will require a computation of the contributions from parton branching in strongly-interacting matter to the terms in the master factorization formula. This deserves a separate paper and will be one of our future goals.

Acknowledgments

A Anomalous dimensions

The RG equation of the hard function is

$$\frac{d}{d\ln\mu}\ln H(Q^2,\mu) \equiv \Gamma_h = 2C_F\gamma_{\rm cusp}\ln\frac{Q^2}{\mu^2} + 2\gamma_q. \tag{A.1}$$

$\gamma_{\rm cusp}$ up to four loops and γ_q up to three loops were collected in ref. [72] and references therein. The RG equation of the beam/jet function reads

$$\frac{d}{d\ln\mu}\ln\mathcal{G}_i = -C_F\gamma_{\rm cusp}\ln\frac{4E_i^2}{\nu^2} + \gamma_{G,i}\,, \tag{A.2}$$

where $\mathcal{G}$ represents the beam function B or the jet function J. E_i is the energy of parton i. The RG equation of the soft function is given by

$$\frac{d}{d\ln\mu}\ln S \equiv \Gamma_s = -2C_F\gamma_{\rm cusp}\ln\frac{\nu^2 n_2\cdot n_4}{2\mu^2} - 2\gamma_s\,. \tag{A.3}$$

The expressions for γ_s up to three loops can be found in refs. [26, 49]. Additionally we have $\gamma_{B,q} = \gamma_{J,q}$, which can be derived from $2\gamma_q + \gamma_{B,q} + \gamma_{J,q} - 2\gamma_s = 0$ according to the scale invariance of the cross sections. Note that

$$2\ln\frac{Q^2}{\mu^2} - \ln\frac{4E_2^2}{\nu^2} - \ln\frac{4E_4^2}{\nu^2} - 2\ln\frac{\nu^2 n_2\cdot n_4}{2\mu^2} = 0\,, \tag{A.4}$$

with $Q^2 = 4E_2 E_4 \frac{n_2\cdot n_4}{2}$.

The rapidity evolution equation of the beam/jet function reads

$$\frac{d}{d\ln\nu}\ln\mathcal{G}_i = C_F\left[\int_{b_0^2/b^2}^{\mu^2}\frac{d\bar{\mu}^2}{\bar{\mu}^2}\gamma_{\rm cusp}(\bar{\mu}) - \gamma_r(b_0^2/b^2)\right]]\,. \tag{A.5}$$

Similarly, the rapidity evolution equation of the soft function is given by

$$\frac{d}{d\ln\nu}\ln S = 2C_F\left[-\int_{b_0^2/b^2}^{\mu^2}\frac{d\bar{\mu}^2}{\bar{\mu}^2}\gamma_{\rm cusp}(\bar{\mu}) + \gamma_r(b_0^2/b^2)\right]\,, \tag{A.6}$$

where γ_r can be found in refs. [26, 49]. The cross section is independent of ν, which leads to the constraint

$$\frac{d}{d\ln\nu}\ln B_q + \frac{d}{d\ln\nu}\ln J_q + \frac{d}{d\ln\nu}\ln S = 0\,. \tag{A.7}$$

References

[1] S. Catani and M.H. Seymour, *A general algorithm for calculating jet cross-sections in NLO QCD*, *Nucl. Phys. B* **485** (1997) 291 [*Erratum ibid.* **510** (1998) 503] [hep-ph/9605323] [INSPIRE].

[2] D. Graudenz, *Disaster++: version* 1.0, `hep-ph/9710244` [InSPIRE].

[3] Z. Nagy and Z. Trócsányi, *Multijet cross-sections in deep inelastic scattering at next-to-leading order*, *Phys. Rev. Lett.* **87** (2001) 082001 [`hep-ph/0104315`] [InSPIRE].

[4] T. Gehrmann, A. Huss, J. Mo and J. Niehues, *Second-order QCD corrections to event shape distributions in deep inelastic scattering*, *Eur. Phys. J. C* **79** (2019) 1022 [`arXiv:1909.02760`] [InSPIRE].

[5] V. Antonelli, M. Dasgupta and G.P. Salam, *Resummation of thrust distributions in DIS*, *JHEP* **02** (2000) 001 [`hep-ph/9912488`] [InSPIRE].

[6] M. Dasgupta and G.P. Salam, *Resummation of the jet broadening in DIS*, *Eur. Phys. J. C* **24** (2002) 213 [`hep-ph/0110213`] [InSPIRE].

[7] M. Dasgupta and G.P. Salam, *Resummed event shape variables in DIS*, *JHEP* **08** (2002) 032 [`hep-ph/0208073`] [InSPIRE].

[8] M. Dasgupta and G.P. Salam, *Event shapes in e^+e^- annihilation and deep inelastic scattering*, *J. Phys. G* **30** (2004) R143 [`hep-ph/0312283`] [InSPIRE].

[9] Z.-B. Kang, X. Liu and S. Mantry, *1-jettiness DIS event shape: NNLL+NLO results*, *Phys. Rev. D* **90** (2014) 014041 [`arXiv:1312.0301`] [InSPIRE].

[10] D. Kang and T. Maji, *Toward precision jet event shape for future electron-ion collider*, `PoS(LC2019)061` (2019) [`arXiv:1912.10656`] [InSPIRE].

[11] D. Kang, C. Lee and I.W. Stewart, *DIS event shape at N^3LL*, `PoS(DIS2015)142` (2015) [InSPIRE].

[12] H1 collaboration, *Measurement of event shape variables in deep inelastic ep scattering*, *Phys. Lett. B* **406** (1997) 256 [`hep-ex/9706002`] [InSPIRE].

[13] ZEUS collaboration, *Event shape analysis of deep inelastic scattering events with a large rapidity gap at HERA*, *Phys. Lett. B* **421** (1998) 368 [`hep-ex/9710027`] [InSPIRE].

[14] H1 collaboration, *Investigation of power corrections to event shape variables measured in deep inelastic scattering*, *Eur. Phys. J. C* **14** (2000) 255 [*Erratum ibid.* **18** (2000) 417] [`hep-ex/9912052`] [InSPIRE].

[15] ZEUS collaboration, *Measurement of event shapes in deep inelastic scattering at HERA*, *Eur. Phys. J. C* **27** (2003) 531 [`hep-ex/0211040`] [InSPIRE].

[16] H1 collaboration, *Measurement of event shape variables in deep-inelastic scattering at HERA*, *Eur. Phys. J. C* **46** (2006) 343 [`hep-ex/0512014`] [InSPIRE].

[17] ZEUS collaboration, *Event shapes in deep inelastic scattering at HERA*, *Nucl. Phys. B* **767** (2007) 1 [`hep-ex/0604032`] [InSPIRE].

[18] A. Ali, E. Pietarinen and W. Stirling, *Transverse energy-energy correlations: a test of perturbative QCD for the proton-anti-proton collider*, *Phys. Lett. B* **141** (1984) 447 [InSPIRE].

[19] C. Basham, L.S. Brown, S.D. Ellis and S.T. Love, *Energy correlations in electron-positron annihilation: testing QCD*, *Phys. Rev. Lett.* **41** (1978) 1585 [InSPIRE].

[20] L.J. Dixon, M.-X. Luo, V. Shtabovenko, T.-Z. Yang and H.X. Zhu, *Analytical computation of energy-energy correlation at next-to-leading order in QCD*, *Phys. Rev. Lett.* **120** (2018) 102001 [`arXiv:1801.03219`] [InSPIRE].

[21] M.-X. Luo, V. Shtabovenko, T.-Z. Yang and H.X. Zhu, *Analytic next-to-leading order calculation of energy-energy correlation in gluon-initiated Higgs decays*, *JHEP* **06** (2019) 037 [arXiv:1903.07277] [INSPIRE].

[22] A.V. Belitsky, S. Hohenegger, G.P. Korchemsky, E. Sokatchev and A. Zhiboedov, *From correlation functions to event shapes*, *Nucl. Phys. B* **884** (2014) 305 [arXiv:1309.0769] [INSPIRE].

[23] A.V. Belitsky, S. Hohenegger, G.P. Korchemsky, E. Sokatchev and A. Zhiboedov, *Event shapes in N = 4 super-Yang-Mills theory*, *Nucl. Phys. B* **884** (2014) 206 [arXiv:1309.1424] [INSPIRE].

[24] A.V. Belitsky, S. Hohenegger, G.P. Korchemsky, E. Sokatchev and A. Zhiboedov, *Energy-energy correlations in N = 4 supersymmetric Yang-Mills theory*, *Phys. Rev. Lett.* **112** (2014) 071601 [arXiv:1311.6800] [INSPIRE].

[25] J.M. Henn, E. Sokatchev, K. Yan and A. Zhiboedov, *Energy-energy correlation in N = 4 super Yang-Mills theory at next-to-next-to-leading order*, *Phys. Rev. D* **100** (2019) 036010 [arXiv:1903.05314] [INSPIRE].

[26] I. Moult and H.X. Zhu, *Simplicity from recoil: the three-loop soft function and factorization for the energy-energy correlation*, *JHEP* **08** (2018) 160 [arXiv:1801.02627] [INSPIRE].

[27] L.J. Dixon, I. Moult and H.X. Zhu, *Collinear limit of the energy-energy correlator*, *Phys. Rev. D* **100** (2019) 014009 [arXiv:1905.01310] [INSPIRE].

[28] M. Kologlu, P. Kravchuk, D. Simmons-Duffin and A. Zhiboedov, *The light-ray OPE and conformal colliders*, arXiv:1905.01311 [INSPIRE].

[29] G.P. Korchemsky, *Energy correlations in the end-point region*, *JHEP* **01** (2020) 008 [arXiv:1905.01444] [INSPIRE].

[30] H. Chen, T.-Z. Yang, H.X. Zhu and Y.J. Zhu, *Analytic continuation and reciprocity relation for collinear splitting in QCD*, arXiv:2006.10534 [INSPIRE].

[31] A. Ali, F. Barreiro, J. Llorente and W. Wang, *Transverse energy-energy correlations in next-to-leading order in α_s at the LHC*, *Phys. Rev. D* **86** (2012) 114017 [arXiv:1205.1689] [INSPIRE].

[32] A. Gao, H.T. Li, I. Moult and H.X. Zhu, *Precision QCD event shapes at hadron colliders: the transverse energy-energy correlator in the back-to-back limit*, *Phys. Rev. Lett.* **123** (2019) 062001 [arXiv:1901.04497] [INSPIRE].

[33] A. Gao, H.T. Li, I. Moult and H.X. Zhu, *Hadron collider dijet event shapes at next-to-next-to-next-to-leading logarithm*, in preparation.

[34] C.W. Bauer, D. Pirjol and I.W. Stewart, *Soft collinear factorization in effective field theory*, *Phys. Rev. D* **65** (2002) 054022 [hep-ph/0109045] [INSPIRE].

[35] C.W. Bauer and I.W. Stewart, *Invariant operators in collinear effective theory*, *Phys. Lett. B* **516** (2001) 134 [hep-ph/0107001] [INSPIRE].

[36] C.W. Bauer, S. Fleming, D. Pirjol and I.W. Stewart, *An effective field theory for collinear and soft gluons: heavy to light decays*, *Phys. Rev. D* **63** (2001) 114020 [hep-ph/0011336] [INSPIRE].

[37] C.W. Bauer, S. Fleming and M.E. Luke, *Summing Sudakov logarithms in $B \to X_s\gamma$ in effective field theory*, *Phys. Rev. D* **63** (2000) 014006 [hep-ph/0005275] [INSPIRE].

[38] M. Beneke, A.P. Chapovsky, M. Diehl and T. Feldmann, *Soft collinear effective theory and heavy to light currents beyond leading power*, *Nucl. Phys. B* **643** (2002) 431 [hep-ph/0206152] [INSPIRE].

[39] M.-X. Luo, X. Wang, X. Xu, L.L. Yang, T.-Z. Yang and H.X. Zhu, *Transverse parton distribution and fragmentation functions at NNLO: the quark case*, *JHEP* **10** (2019) 083 [arXiv:1908.03831] [INSPIRE].

[40] M.-X. Luo, T.-Z. Yang, H.X. Zhu and Y.J. Zhu, *Transverse parton distribution and fragmentation functions at NNLO: the gluon case*, *JHEP* **01** (2020) 040 [arXiv:1909.13820] [INSPIRE].

[41] D. Gutierrez-Reyes, I. Scimemi, W.J. Waalewijn and L. Zoppi, *Transverse momentum dependent distributions in e^+e^- and semi-inclusive deep-inelastic scattering using jets*, *JHEP* **10** (2019) 031 [arXiv:1904.04259] [INSPIRE].

[42] Y. Li, D. Neill and H.X. Zhu, *An exponential regulator for rapidity divergences*, *Nucl. Phys. B* **960** (2020) 115193 [arXiv:1604.00392] [INSPIRE].

[43] T. Gehrmann, T. Lubbert and L.L. Yang, *Transverse parton distribution functions at next-to-next-to-leading order: the quark-to-quark case*, *Phys. Rev. Lett.* **109** (2012) 242003 [arXiv:1209.0682] [INSPIRE].

[44] T. Gehrmann, T. Luebbert and L.L. Yang, *Calculation of the transverse parton distribution functions at next-to-next-to-leading order*, *JHEP* **06** (2014) 155 [arXiv:1403.6451] [INSPIRE].

[45] T. Lübbert, J. Oredsson and M. Stahlhofen, *Rapidity renormalized TMD soft and beam functions at two loops*, *JHEP* **03** (2016) 168 [arXiv:1602.01829] [INSPIRE].

[46] M.G. Echevarria, I. Scimemi and A. Vladimirov, *Unpolarized transverse momentum dependent parton distribution and fragmentation functions at next-to-next-to-leading order*, *JHEP* **09** (2016) 004 [arXiv:1604.07869] [INSPIRE].

[47] M.-X. Luo, T.-Z. Yang, H.X. Zhu and Y.J. Zhu, *Quark transverse parton distribution at the next-to-next-to-next-to-leading order*, *Phys. Rev. Lett.* **124** (2020) 092001 [arXiv:1912.05778] [INSPIRE].

[48] M.G. Echevarria, I. Scimemi and A. Vladimirov, *Transverse momentum dependent fragmentation function at next-to-next-to-leading order*, *Phys. Rev. D* **93** (2016) 011502 [*Erratum ibid.* **94** (2016) 099904] [arXiv:1509.06392] [INSPIRE].

[49] Y. Li and H.X. Zhu, *Bootstrapping rapidity anomalous dimensions for transverse-momentum resummation*, *Phys. Rev. Lett.* **118** (2017) 022004 [arXiv:1604.01404] [INSPIRE].

[50] T. Becher, M. Neubert and B.D. Pecjak, *Factorization and momentum-space resummation in deep-inelastic scattering*, *JHEP* **01** (2007) 076 [hep-ph/0607228] [INSPIRE].

[51] P.A. Baikov, K.G. Chetyrkin, A.V. Smirnov, V.A. Smirnov and M. Steinhauser, *Quark and gluon form factors to three loops*, *Phys. Rev. Lett.* **102** (2009) 212002 [arXiv:0902.3519] [INSPIRE].

[52] T. Gehrmann, E.W.N. Glover, T. Huber, N. Ikizlerli and C. Studerus, *Calculation of the quark and gluon form factors to three loops in QCD*, *JHEP* **06** (2010) 094 [arXiv:1004.3653] [INSPIRE].

[53] E.C. Aschenauer et al., *eRHIC design study: an electron-ion collider at BNL*, arXiv:1409.1633 [INSPIRE].

[54] J. Butterworth et al., *PDF4LHC recommendations for LHC run II*, *J. Phys. G* **43** (2016) 023001 [arXiv:1510.03865] [InSPIRE].

[55] S. Dulat et al., *New parton distribution functions from a global analysis of quantum chromodynamics*, *Phys. Rev. D* **93** (2016) 033006 [arXiv:1506.07443] [InSPIRE].

[56] L.A. Harland-Lang, A.D. Martin, P. Motylinski and R.S. Thorne, *Parton distributions in the LHC era: MMHT 2014 PDFs*, *Eur. Phys. J. C* **75** (2015) 204 [arXiv:1412.3989] [InSPIRE].

[57] NNPDF collaboration, *Parton distributions for the LHC run II*, *JHEP* **04** (2015) 040 [arXiv:1410.8849] [InSPIRE].

[58] A. Buckley et al., *LHAPDF6: parton density access in the LHC precision era*, *Eur. Phys. J. C* **75** (2015) 132 [arXiv:1412.7420] [InSPIRE].

[59] T. Sjöstrand, S. Mrenna and P.Z. Skands, *A brief introduction to PYTHIA 8.1*, *Comput. Phys. Commun.* **178** (2008) 852 [arXiv:0710.3820] [InSPIRE].

[60] T. Sjöstrand et al., *An introduction to PYTHIA 8.2*, *Comput. Phys. Commun.* **191** (2015) 159 [arXiv:1410.3012] [InSPIRE].

[61] Z. Nagy and Z. Trócsányi, *Three-jet event-shapes in lepton-proton scattering at next-to-leading order accuracy*, *Phys. Lett. B* **634** (2006) 498 [hep-ph/0511328] [InSPIRE].

[62] J.C. Collins and D.E. Soper, *Back-to-back jets: Fourier transform from B to k-transverse*, *Nucl. Phys. B* **197** (1982) 446 [InSPIRE].

[63] Y.L. Dokshitzer, G. Marchesini and B.R. Webber, *Nonperturbative effects in the energy energy correlation*, *JHEP* **07** (1999) 012 [hep-ph/9905339] [InSPIRE].

[64] P. Sun, J. Isaacson, C.P. Yuan and F. Yuan, *Nonperturbative functions for SIDIS and Drell-Yan processes*, *Int. J. Mod. Phys. A* **33** (2018) 1841006 [arXiv:1406.3073] [InSPIRE].

[65] A. Prokudin, P. Sun and F. Yuan, *Scheme dependence and transverse momentum distribution interpretation of Collins-Soper-Sterman resummation*, *Phys. Lett. B* **750** (2015) 533 [arXiv:1505.05588] [InSPIRE].

[66] X. Li et al., *A new heavy flavor program for the future electron-ion collider*, *EPJ Web Conf.* **235** (2020) 04002 [arXiv:2002.05880] [InSPIRE].

[67] G. Ovanesyan and I. Vitev, *An effective theory for jet propagation in dense QCD matter: jet broadening and medium-induced bremsstrahlung*, *JHEP* **06** (2011) 080 [arXiv:1103.1074] [InSPIRE].

[68] Z.-B. Kang, F. Ringer and I. Vitev, *Effective field theory approach to open heavy flavor production in heavy-ion collisions*, *JHEP* **03** (2017) 146 [arXiv:1610.02043] [InSPIRE].

[69] H.T. Li and I. Vitev, *Inclusive heavy flavor jet production with semi-inclusive jet functions: from proton to heavy-ion collisions*, *JHEP* **07** (2019) 148 [arXiv:1811.07905] [InSPIRE].

[70] H.T. Li and I. Vitev, *Inverting the mass hierarchy of jet quenching effects with prompt b-jet substructure*, *Phys. Lett. B* **793** (2019) 259 [arXiv:1801.00008] [InSPIRE].

[71] H.T. Li and I. Vitev, *Jet charge modification in dense QCD matter*, *Phys. Rev. D* **101** (2020) 076020 [arXiv:1908.06979] [InSPIRE].

[72] T. Becher and M. Neubert, *Infrared singularities of scattering amplitudes and N^3LL resummation for n-jet processes*, *JHEP* **01** (2020) 025 [arXiv:1908.11379] [InSPIRE].